




RESEARCH ARTICLE

# Canopy development, leaf traits and yield in high-altitude Andean maize under contrasting plant densities in Argentina

D. A. Salve<sup>1</sup>, M. L. Maydup<sup>2</sup>, G. A. Salazar<sup>3</sup>, E. A. Tambussi<sup>2</sup> and M. Antonietta<sup>2</sup> 

<sup>1</sup>INTA IPAF Región NOA, Posta de Hornillos, Argentina, <sup>2</sup>Instituto de Fisiología Vegetal (INFIVE, CONICET-UNLP), La Plata, Argentina and <sup>3</sup>Instituto de Investigaciones en Energía No Convencional (INENCO, CONICET-UNSa), Salta, Argentina

**Corresponding author:** M. Antonietta; Email: [antoniettamariana@gmail.com](mailto:antoniettamariana@gmail.com)

(Received 05 July 2023; revised 17 October 2023; accepted 20 October 2023)

## Summary

In highlands, the increase in altitude results in a drastic decrease in temperature (T) that delays phenological development of maize, decreasing light interception during the cycle. This could be partially overcome by increasing plant density, but information is scarce for designing specific management options. The objective of this work was to describe changes in canopy development, photosynthetic performance, biomass and yield of maize grown at contrasting plant densities (5.7 plants m<sup>-2</sup>, locally used, and 8.7 plants m<sup>-2</sup>, 50% higher). Three experiments were carried out in two high-altitude environments within the Argentinean Andean region, Hornillos (HOR, 2380 masl, 2019–20 and 2020–21) and El Rosal (ERO, 3350 masl, 2019–20), and complementary data were obtained from samplings in 8 farmer's fields (from 2400 to 3400 masl, 2022–23). In the experiments, mean T during the first 150 days of the cycle was 33% lower at ERO, which implied 39 extra days but 25% shorter thermal time to achieve silking. The higher plant density significantly increased leaf area index and light interception at ERO, whereas at HOR, this was only evident during the second season. At the leaf level, plants grown at ERO had thicker leaves with higher chlorophyll (+36%) and nitrogen (40%) content. Photosynthetic electron transport rate at full irradiance was +20% higher at ERO but significantly varied throughout the day with lowest values in the morning, which was not observed at HOR and was not related to light intensity or stomatal conductance. At HOR, the increase in plant density did not improve light interception, nor yield in 2019–20 (with average yields of 6356 kg ha<sup>-1</sup>) but it did improve both in 2020–21 when generally lower yields were attained (4821 kg ha<sup>-1</sup>). Across farmer's fields, increasing densities consistently reduced yield per plant ( $r^2 = 0.57^{***}$ ) but improved yield per area basis, which was maximised at 10 pl m<sup>-2</sup> as a result of a steady increase in kernel number m<sup>-2</sup> (up to 15 pl m<sup>-2</sup>). Thus, in these high-altitude environments, increasing plant density beyond recommended (6 pl m<sup>-2</sup>) is a promising approach for improving yield, with major penalties of supra-optimum densities being related to kernel weight. Further work is needed to explore the effect of different factors limiting kernel growth, over plant density responses.

**Keywords:** *Zea mays*; highlands; kernel number; kernel weight; biomass

## Introduction

Worldwide, family and indigenous agriculture provide around 56% of basic food products but occupy barely 20% of the available arable land (Gornitzky, 2015), most of which is marginal in terms of yield potential of main crops. In the Northwest of Argentina (NWA), yields are limited by the natural conditions of the highlands (those located at least 1000 metres above the sea level, masl) characterised by low air temperature (T), which decreases with an average rate of 0.55°C for

every 100 m (Körner, 2003). On the contrary, in the NWA, solar radiation can be 30% higher during summer at 3350 compared with 1150 masl in locations at similar latitudes, partly due to increased UV (Utrillas *et al.*, 2018). Most cropped species in the NWA are maize, quinoa and Andean potato ([www.siaa.gov.ar](http://www.siaa.gov.ar)) among which maize is the only one with a C<sub>4</sub> photosynthetic metabolism, implying higher sensibility to low T but, at the same time, a higher response to increasing irradiances (Andrade, 1995; Muchow *et al.*, 1990). Available information regarding the compound effects of altitude on maize crops is scarce, and more studies are needed to develop specific management strategies for maize in these environments.

At increasing altitudes, the decrease in mean T implies a shortening of the frost-free period and a concomitant delay in sowing date, which reduces the crop cycle duration and, with this, the light interception throughout it. After sowing, low temperatures extend the duration in days of phenological stages (Ritchie and Hanway, 1989), with differences of up to 80 days in crop cycle duration between sites differing in 1000 m of altitude (Cooper, 1979). This implies a delay in achieving maximum leaf area index (LAI), resulting in further reductions in light interception and biomass accumulation with increasing altitude (Cooper, 1979; Pace, 2019). At the same time, the decrease in T with increasing altitude will also extend the duration of the critical period, and with this, the light interception during this period could finally result in a larger grain number (Andrade *et al.*, 1999). Consistently, increasing night T during the critical period (+5°C with maximum night T of 25°C) results in a shortening of this stage and a lower grain number (Cantarero *et al.*, 1999).

Among the environmental factors affecting photosynthesis, low night temperatures can reduce maize photosynthesis by up to 30%, especially in the early morning (Kosová *et al.*, 2005; Ying *et al.*, 2000). Also, the lower atmospheric pressure typical of high-altitude environments can reduce the CO<sub>2</sub> diffusion rates to chloroplasts (Körner, 2007) and lower vapour pressure deficits (typical in the NWA) may promote stomatal closure regardless of the plant water status, implying CO<sub>2</sub> limitations for photosynthesis even in C<sub>4</sub> species (Hirasawa y Hsiao, 1999). On the other hand, higher irradiance with increasing altitude could represent an advantage for maize, whose photosynthesis at the leaf level saturates beyond 2000 μmoles photons m<sup>-2</sup> s<sup>-1</sup> (Chen *et al.*, 2014).

Part of these negative environmental effects could be mitigated by increasing plant density, which is an important management variable in maize (Maddonni *et al.*, 2001; Tokatlidis and Koutroubas, 2004). A higher plant density could partially overcome the delayed crop phenology, allowing an earlier achievement of maximum leaf area index further benefitted from the larger radiation input, whereas detrimental effects over grain number could be compensated for by an extended duration of the critical period. The objective of this work is to evaluate canopy development, light interception, leaf traits, photosynthetic performance and yield of Andean maize cropped in highlands under contrasting plant densities.

## Materials and Methods

### Experimental design

Experiments were conducted in two sites of NWA located at different altitudes. One of the sites was in Hornillos (hereafter, HOR), Jujuy province, at 2380 masl (23.65° S. 65.43° W) within the Instituto de Investigación y Desarrollo Tecnológico para la Agricultura Familiar del Noroeste Argentino, IPAF NOA (Institute for Smallholders Agriculture of the Northwest of Argentina), which belongs to the Instituto Nacional de Tecnología Agropecuaria, INTA (National Institute of Agricultural Technology). The other site was in an annexed field of the elementary school at El Rosal (hereafter, ERO), Salta province, at 3350 masl (24.38° S. 65.77° W). At each site, treatments consisted of two contrasting planting densities: 5.7 and 8.6 plants m<sup>-2</sup>. The low density corresponded to the recommended density for these environments (Gómez and Macedo, 2011) whereas 8.6 plants m<sup>-2</sup> is 50% higher than recommended. An open-pollinated line called 'creole

yellow corn' was sown at both sites and 'white corn' was also included at HOR. Both genotypes are usually cropped by farmers within this altitudinal range and have been widely known as local races (Cámara Hernández *et al.*, 2011). Seeds were obtained from the INTA seed multiplication programme. Soil samples were taken at each site and classified as sandy loam at HOR and sandy at ERO (Suppl. Material Table S1). Both soils had high values of organic matter (>2.8%), and similar pH values and carbon/N relationships.

### **Crop management**

Previous crop was Andean potato at ERO, quinoa and amaranth at HOR in the first season and maize at HOR in the second season. Approximately 30 days before sowing, dry goat guano was applied at an estimated rate of 1 kg m<sup>-2</sup> in both sites, which is similar to rates used by local farmers (Gómez and Macedo, 2011). Guano chemical composition was analysed in 2019 in the laboratory of the Universidad Nacional de Jujuy (National University of Jujuy), allowing to estimated rate of 187 kg ha<sup>-1</sup> of nitrogen and 174 ppm of extractable phosphorus applied. Treatments were laid out in three blocks (four blocks in HOR in the second season) and densities were randomly distributed in plots within each block at each site. At HOR, genotypes were distributed in subplots within each plant density. Each plot (ERO) or subplot (HOR) consisted of 4 rows 0.7 m apart and 4 m long (11.2 m<sup>2</sup>). Seeds were sown manually on October 29<sup>th</sup> at HOR, October 31<sup>st</sup> at ERO in 2019 and December 2<sup>nd</sup> at HOR in 2020. Three seeds were placed on each hill and then thinned to the aimed density after emergence. The crop was maintained free of weeds and insects using conventional agrochemicals when necessary and was irrigated as needed from emergence using ditch irrigation at HOR and drip irrigation at ERO. Previous work indicates that nitrogen leaching is higher under ditch irrigation and water use efficiency is lower compared with drip irrigation (Li *et al.*, 2020). However, these effects can be negligible in our work, since organic fertiliser was used (less prone to leaching) and water offered was enough to prevent water stress symptoms throughout the cycle.

### **Meteorological conditions**

At HOR, T was registered by a meteorological station 100 m away from the experimental field. At ERO, T was registered by a thermocouple placed in a meteorological shelter; however, due to technical problems, gaps arose in the series of measured data. To fill these gaps, the hourly values estimated by the SOLCAST satellite database (<https://solcast.com/>) have been used, after a correction by linear approximation based on correlations between measured hourly T values and the SOLCAST values (only valid for summertime):

$$T_{\text{ERO}}(^{\circ}\text{C}) = 1.56 * T_{\text{SOLCAST}}(^{\circ}\text{C}) - 1.37 \quad (1)$$

Solar radiation was also estimated using the SOLCAST model. Thermal time computations started at sowing, using mean daily air T and a base T of 8°C (Ritchie and NeSmith, 1991) whereas mean temperatures never exceeded the optimum T for maize growth (34°C, Wilkens and Singh, 2003). Thus, we used a simple linear model to calculate thermal time, which was expressed as the sum of °C day<sup>-1</sup> (Cd).

### **Non-Destructive determinations**

In each site, 6 consecutive plants within the central rows of each plot were tagged at the V3 stage for non-destructive determinations. Crop phenology was determined in the tagged plants following the scale proposed by Ritchie and Hanway (1989). Leaf area was assessed non-destructively by measuring the maximum length and width of each leaf and multiplying it by 0.75 as in Montgomery (1911) so that:

$$\text{Individual leaf area} = \text{length} \times \text{width} \times 0.75. \quad (2)$$

LAI was then calculated as the sum of the area of all the leaves of each plant multiplied by plant density. After flowering, a visual register of canopy senescence was done weekly and the area of senesced leaves (with more than 50% of its area yellowed) was subtracted from the LAI maximum achieved at flowering.

### **Chlorophyll content, specific leaf area and leaf N content**

Different leaf traits were measured in leaves representing different canopy positions. The leaves measured were the third leaf above the main ear, representing an apical leaf, the leaf adjacent to the ear, representing a middle-positioned leaf, and the leaf positioned three leaves below the ear leaf, representing a basal leaf. In some plants, the earbud was still not visible by the time of sampling; in these cases the leaf below the topper-most expanded leaf was considered the apical leaf, going downwards every 3 nodes for middle and basal leaves. Chlorophyll content was assessed using a SPAD 502 (Minolta, EEUU). At least five measurements across the leaf blade were made and averaged, and three plants per plot (9 plants per treatment) were measured.

In these same leaf positions, specific leaf area was determined by punching 6 cm<sup>2</sup> at the mid-third of each leaf thrice (*i.e.*, 18 cm<sup>2</sup> per leaf). Samples were obtained from 2 plants per plot (6 plants per treatment). Leaf discs were dried in an oven at 60°C until constant weight and weighed. Specific leaf area was calculated as the quotient between the area of each leaf sample and the respective dry weight.

After specific leaf area was assessed, the same samples were utilised to determine leaf N content. A compound sample obtained from 2 plants per plot (3 replicates per each site × plant density × leaf position combination) was used for micro-Kjeldahl analyses using Hanon equipment (Nade, K9840) following conventional protocols for digestion and distillation of the samples.

### **Chlorophyll fluorescence measurements and stomatal conductance**

Simultaneous photosynthetic electron transport rate (ETR) and stomatal conductance (gs) measurements were taken during 2 clear-sky days and at three times during the day: morning (09:00–11:00 hs), midday (12:00–14:00 hs) and afternoon (15:00–17:00 hs). Measurements were taken in apical, middle and basal leaves, representing different positions within the canopy (see above).

The effective photosystem II quantum yield was measured using a pulse-amplitude-modulated FMS2 chlorophyll fluorometer (Hansatech, UK). Each measurement was done in 3 plants per plot (9 plants per treatment) in fully illuminated spots around the middle position of the leaf lamina between the midrib and the leaf margin. Thus, measurements are an estimation of the photosynthetic potential of each leaf at each time of the day but do not account for differences related to varying irradiances throughout the day or across the canopy. Linear electron transport rate was calculated as in Rosenqvist and van Kooten (2003):

$$\text{ETR} = \text{PPFD} \times \text{abs} \times \phi\text{PSII} \times 0.5 \quad (3)$$

where PPFD is the Photosynthetic Photon Flux Density, abs is leaf absorptance (0.8),  $\phi\text{PSII}$  is effective photosystem II quantum yield and 0.5 is a factor considering that 2 photons are absorbed by each transported electron (and assuming a 1:1 photosystem II/photosystem I ratio). The factor 0.8 (leaf absorptance) is typical for non-senescent leaves of maize (Acciaresi *et al.*, 2014).

Stomatal conductance measurements were taken with a Porometer SC-1 (Decagon, USA) on the abaxial side of the leaf, in the same fully illuminated leaf spots used for ETR measurements.

### **Biomass, yield and yield components**

In both seasons, destructive samplings were made at HOR at physiological maturity for dry matter determinations. In each subplot, 6 previously tagged plants were harvested and dissected in three parts: (i) stalks with leaf sheaths and tassels, (ii) leaf blades and (iii) ears. All parts were dried in a forced-air oven at 60°C to constant weight and weighed. Aboveground plant biomass was estimated as the sum of stalks, leaf blades and ears.

Yield was estimated by harvesting 20 ears from consecutive plants within the central rows of each plot. No barren plants were found in any of the experiments. Ears were threshed manually, grains were weighed and an aliquot was oven-dried to constant weight to calculate the percentage of grain moisture in order to express yield at 0% moisture. Mean individual kernel weight (KW) was estimated by counting and weighting grains of each plant harvested for biomass. Kernel number per plant (KNP) was estimated on the basis of KW and grain yield of 20 plants per plot.

### **Samplings in farmer's fields**

To complement the experimental results, during the 2022–23 growing season, samplings were carried out in 8 farmer's fields across an altitudinal gradient spanning from 2400 up to 3400 masl, and within  $-23.20^\circ$  and  $-24.41^\circ$  latitude (Fig. S1). In all cases, yellow or white maize varieties were sown at conventional sowing dates, irrigated by furrow irrigation and fertilised with goat manure, and no evidence of nutritional or drought stress was observed by the time of visiting the fields. In each field, two separate plots with 4 rows and 1.5 m length were identified around flowering, aiming to represent a variation of plant densities. Plant density was separately estimated for each of the central rows of each plot by counting the total number of plants in the harvested row and the adjacent rows at each side and dividing it by the area occupied by these plants (i.e.,  $1.5 \text{ m length} \times 0.70 \text{ distance between rows} \times 3 \text{ rows}$ ). At maturity, all the ears in each of the central rows of each plot were separately harvested, threshed manually, dried until constant weight and weighed. The number of grains per ear was counted and the kernel weight was estimated on the basis of yield per plant and KNP. Thus, a maximum of 4 data of yield and plant density was available in each farmer field although for different reasons (usually bird attack) some plots were lost in some fields.

### **Statistical analyses**

Data were analysed using the STATISTICA 7.1 Software (Stat-Soft, Inc., Tulsa, Oklahoma, USA). Treatments and interaction between them were analysed by ANOVA, and the Levene's test was used to corroborate the assumptions of the model. Each site was analysed independently because of different measurement times except when specifically stated. Plant density, genotype (at HOR) and block were considered fixed factors and each independent variable was analysed separately. For variables comprising different leaves of the canopy or different moments during the day, the leaf position and/or the moment of the day were also treated as fixed factors. When interaction among factors was detected, the LSD test ( $p < 0.05$ ) was used to identify homogenous groups. The significance of regressions was assessed through the *F*-test ( $p < 0.05$ ).

## **Results**

### **Environmental variation and phenological development**

The increase in altitude from 2380 masl at HOR to 3350 at ERO implied an important decrease in *T*. During 2019–20, medium *T* during the first 150 days of the cycle was 33% higher at HOR compared with ERO (Fig. 1a, b) whereas differences in minimum *T* were even larger (+40% at HOR). Regarding chilling stress ( $<10^\circ\text{C}$ , Waqas *et al.*, 2021), during the first 150 days of the cycle,

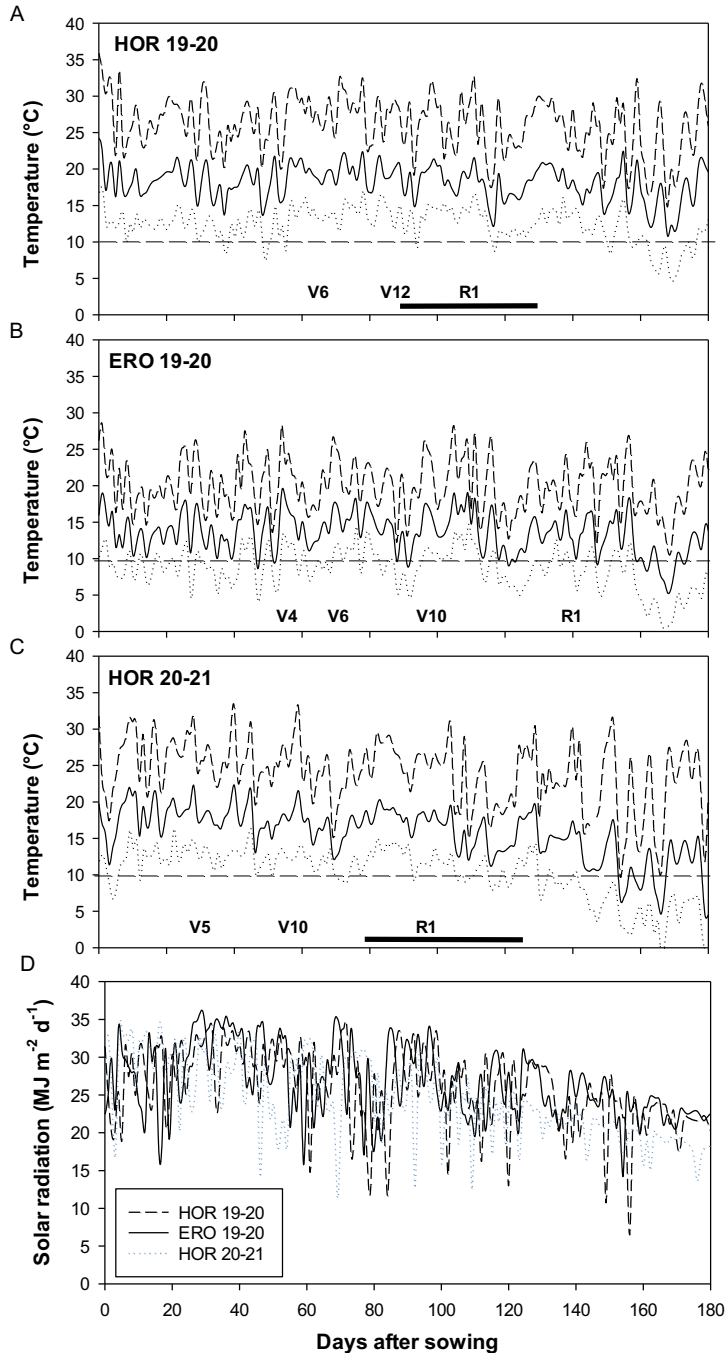


**Figure 1.** Temperatures during the growing cycle of Andean maize in Hornillos (2380 masl) during 2019–20 (A) and 2020–21 (C) and in El Rosal (3350 masl) during 2019–20 (B), and solar radiation ( $\text{MJ m}^{-2}$ ) in the three experiments estimated by the SOLCAST satellite database (D). Minimum, mean and maximum temperatures are indicated by dotted, solid and dashed lines, respectively, and the horizontal dashed lines mark the limit for temperatures below  $10^{\circ}\text{C}$ , potentially stressful for maize. Phenological stages, indicated above the 'x' axis, are defined based on the scale proposed by Ritchie *et al.* (1989). In Figures A and C, the black bar below R1 indicates the chronological time elapsed during the critical period estimated in  $400^{\circ}\text{C}$  bracketing silking (Sadras and Calderini, 2020).

only 7 days with minimum T below 10°C were registered at HOR whereas, at ERO, there were 94 days out of 150 with minimum T below 10°C. Thus, at ERO, apart from lower medium T, plants may have also experienced critically low minimum temperatures. As expected, T differences delayed phenological development at the highest altitude site, ERO, where the crop reached silking 39 days later than at HOR in 2019–20 (Fig. 1a, b). Nonetheless, much lower thermal time was required to achieve a given phenological stage at ERO: for example, V6 was reached at 697°C.d at HOR but at 458°C.d at ERO. Thus, thermal time requirements were reduced when lower temperatures were experienced.

Comparing both seasons at HOR, medium and minimum T were higher during the 2019–20 growing season compared with 2020–21, and this was accentuated during the reproductive stage (+16 and +22% higher medium and minimum T in 2019–20 averaged from silking until 40 days after silking, Fig. 1a, c). Cumulative solar radiation was also higher in the 2019–20 growing season, with 11% higher solar radiation accumulated until silking and 8% higher solar radiation accumulated from silking until maturity (Fig. 1d).

### Leaf area index and light interception

The increase in plant density increased LAI and light interception with varying intensity depending on the environment. During the first season at HOR, no significant effect of plant density was detected for LAI or light interception at 86 DAS (Fig. 2a), except for a minor advantage at 65 DAS (+17% higher LAI at high density,  $p < 0.1$ , not shown). By contrast, at ERO, the increase in plant density improved LAI by 75 DAS resulting in a 40% increase in light interception (Fig. 2b). Overall, individual leaf size was larger at ERO compared with HOR (Fig. S2), with a declining trend towards later-developed leaves. Thus, the increase in altitude drastically reduced the LAI achieved by the crop, but this was partially offset by the increase in plant density.

During the 2020–21 growing season at HOR, the higher plant density significantly increased LAI of both genotypes from 28 DAS to 153 DAS (Fig. 2c). In relative terms, this increase was higher during early crop stages (>50% higher LAI until 50 DAS), was maintained around 40% thereafter and tend to diminish towards the end of the growing period due to more accelerated canopy senescence at higher plant density. Light interception at midday was significantly improved by plant density until 78 DAS, with no significant effects thereafter. This is consistent with the crop achieving LAI close to 4 by 80 DAS at the lower plant density, which is usually considered a critical value to maximise light interception in maize. Comparing genotypes, white corn achieved significantly higher LAI from 70 DAS onwards, regardless of plant density. However, light interception was slightly but significantly higher in yellow corn, from 64 DAS to 96 DAS, which related to a more planophile leaf habit in yellow corn (Fig. S3). Thus, increasing plant density beyond values conventionally used by farmers resulted in an important increase in LAI and light interception during early stages at ERO (3300 masl) and at HOR during 2020–21, but not at HOR during 2019–20 where highest temperatures during the vegetative period were experienced.

### Leaf traits

Different leaf traits were analysed in 2019–20 around 96–98 DAS at both sites, allowing a representative statistical comparison. Specific leaf area differed between sites depending on the plant density, being significantly higher at HOR at high plant density with no differences between sites at low density (Table 1). The increase in plant density resulted in higher specific leaf area at HOR (*i.e.*, thinner leaves), but, surprisingly, the opposite was true at ERO. Differences were also detected depending on the leaf position with generally higher specific leaf area at basal leaves (Table 1).

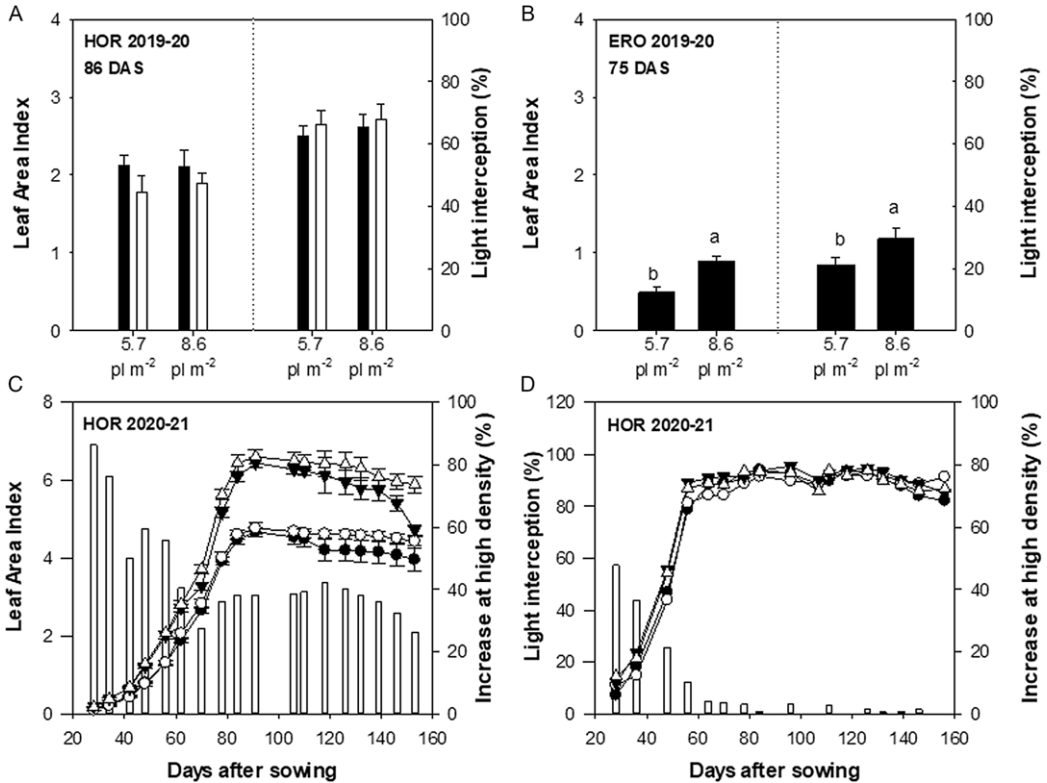


**Figure 2.** Leaf area index and light interception measured at midday in Andean maize at Hornillos (2380 masl) during 2019–20 (A) and 2020–21 (C, D) and at El Rosal (3350 masl) during 2019–20 (B) at different plant densities. In (A), measurements were done 86 days after silking (filled bars correspond to yellow corn, empty bars to white corn). In (B), measurements were done at 75 days after silking in yellow corn. In (C) and (D), circles denote low plant density (5.7 plants m<sup>-2</sup>), triangles denote high plant density (8.6 plants m<sup>-2</sup>), filled symbols denote yellow corn and empty symbols denote white corn. In (C) and (D), empty bars show the relative increase at high plant density compared with low plant density in both genotypes (as no density × genotype interaction for LAI or light interception).

Leaf chlorophyll content was estimated on the basis of SPAD values (‘greenness’) and resembled the differences found for specific leaf area. Significantly higher SPAD values were achieved at ERO (in line with thicker leaves), whereas at HOR, the increase in plant density further reduced SPAD values, consistent with the increase in specific leaf area (*i.e.*, thinner leaves) (Table 1). The SPAD value also changed significantly depending on the leaf position with generally lower SPAD values in apical leaves compared with leaves in middle or basal positions at both sites (Table 1).

Leaf %N and leaf N content were also significantly higher at ERO, with no interaction with plant density (Table 1). While higher leaf N content could be partially attributed to thicker leaves at ERO (+8% compared with HOR), relative differences were much greater for N content (+39% compared with HOR). At both sites, apical and middle-positioned leaves had higher N content than basal leaves (Table 1). Overall, several leaf traits differed between sites with a trend to thicker leaves, with higher chlorophyll and N content at the higher altitude site.

### **Photosynthetic rates and stomatal conductance**

ETR and stomatal conductance (gs) were measured throughout the day in illuminated leaf spots of 3 leaves representing different positions within the canopy. Because ETR values are usually related



**Table 1.** Specific leaf area ( $\text{cm}^2 \text{mg}_{\text{DW}}^{-1}$ ), SPAD values, N concentration (%) and N content ( $\text{mg cm}^{-2}$ ) of Andean maize at two locations: Hornillos (HOR, 2380 masl) and El Rosal (ERO, 3350 masl) during 2019–20. Leaf traits were measured under two contrasting plant densities (5.7 and 8.6  $\text{pl m}^{-2}$ ), in 3 leaves representing different positions within the canopy (basal, mid and apical leaves). Statistical significance represented as \*:  $p < 0.05$ ; \*\*:  $p < 0.01$  and \*\*\*:  $p < 0.001$ ; NS indicates no significant relationship. For each trait, mean values for each significant factor are deployed

	Specific leaf area ( $\text{cm}^2 \text{mg}_{\text{DW}}^{-1}$ )	SPAD values	N concentration (%)	N content ( $\text{mg cm}^{-2}$ )
<i>Location</i>				
HOR	0.196 a	38.3 b	2.2 a	0.121 b
ERO	0.180 b	52.1 a	3.3 b	0.169 a
<i>Plant density</i>				
5.7	0.185	46.9 a	2.7	0.149
8.6	0.191	43.6 b	2.7	0.141
<i>Leaf position</i>				
Lower	0.198 a	46.4 a	2.7	0.135 b
Mid	0.182 b	47.5 a	2.7	0.150 a
Apical	0.183 b	41.7 b	2.8	0.151 a
<i>Location × Plant density</i>				
HOR 5.7	0.183 bc	42.8 b	2.2	0.122
8.6	0.208 a	33.8 c	2.1	0.120
ERO 5.7	0.186 b	51.0 a	3.2	0.177
8.6	0.174 c	53.3 a	3.3	0.160
<i>Location</i>	***	***	***	***
<i>Plant density</i>	NS	**	NS	NS
<i>Leaf position</i>	**	***	NS	*
<i>Location × Plant density</i>	***	***	NS	NS
<i>Location × Leaf position</i>	NS	NS	NS	NS
<i>Plant density × Leaf position</i>	NS	NS	NS	NS
<i>Location × Pl dens × Leaf position</i>	NS	NS	NS	NS

to the incoming photosynthetically active radiation (PAR) at the site of measurement, PAR values were also registered but are not representative of the zenithal incoming PAR at those canopy levels or times of the day. Throughout the day, no variation was found at HOR (Fig. 3a) whereas at ERO, ETR was significantly lower in the morning, increasing by 15% at midday and by 37% in the afternoon, with no evident relationship with PAR (Fig. 3c). Regarding the leaf position, at HOR, ETR was significantly lower in the basal leaf at high plant density (72 vs. 99  $\mu\text{moles e}^- \text{m}^{-2} \text{s}^{-1}$  for the rest of the leaves) but, except for this, no significant differences were detected between leaves, despite slightly higher (+11%) incoming PAR at basal and middle leaves (Fig. 3b). By contrast, at ERO, ETR was +19% higher in basal and middle leaves compared with apical leaves, which may partially relate to their +6% higher incoming PAR (Fig. 3d), likely related to the usually more planophile leaf angle. Comparing sites, ETR was higher at ERO than at HOR, especially at midday (+23%) and in the afternoon (+34%), and especially in low (+30%) and middle-positioned leaves (+24%) (based on comparisons in Fig. 3). Overall, a higher photosynthetic potential was achieved at ERO but also a much higher variation throughout the day.

Stomatal conductance varied throughout the day at both sites. At HOR,  $g_s$  was +44% higher in the morning than later in the day (Fig. 4a) with no apparent effect on ETR, which was unchanged throughout the day (Fig. 3a). Similarly, at ERO,  $g_s$  decreased throughout the day with +53% higher  $g_s$  at the morning and midday compared with the afternoon (Fig. 4c), with no evident relationship with ETR, which was highest in the afternoon (Fig. 3c). Regarding leaf position, at HOR,  $g_s$  was +38% higher at mid and apical leaves compared with the basal leaf (Fig. 4b) but all the leaves achieved similar ETR (Fig. 3b). Also at ERO,  $g_s$  was higher (+26%) at mid and apical leaves compared with the basal leaf (Fig. 4d) with no evident relationship with ETR, which was

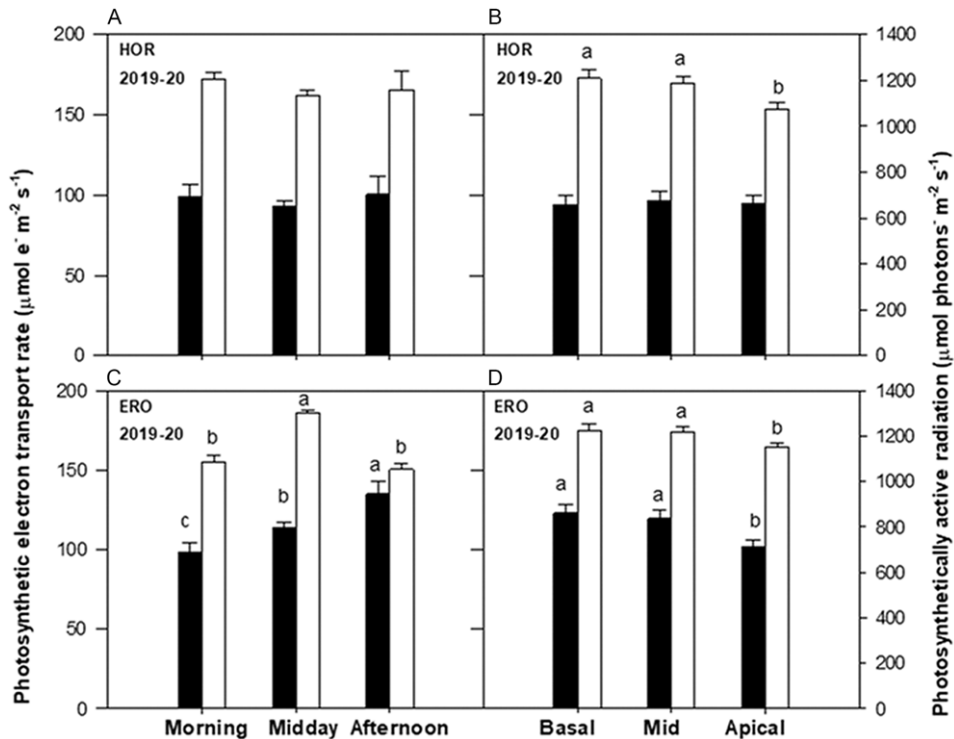


**Figure 3.** Photosynthetic electron transport rate ( $\mu\text{mol e}^- \text{m}^{-2} \text{s}^{-1}$ , filled bars) and photosynthetically active radiation ( $\mu\text{mol photons}^{-1} \text{m}^{-2} \text{s}^{-1}$ , empty bars) at the leaf spot where measurements were taken in Andean maize at Hornillos (2380 masl, a, b) and at El Rosal (3350 masl, c, d) during 2019–20. In each site, measurements were taken during 2 consecutive days, in the morning, midday and afternoon in plants grown under two contrasting plant densities (5.7 plants and 8.6 plants  $\text{m}^{-2}$ ) and in 3 leaves representing different positions within the canopy. Significant differences during the day are shown in A and C by pooling together plant densities and leaf positions, whereas significant differences between leaf positions are shown in B and D by pooling together plant densities and time of the day. Lines above the bars indicate the standard error and letters show homogeneous groups according to the LSD test ( $p < 0.05$ ).

highest in basal and mid leaves (Fig. 3d). Thus, overall, ETR differences throughout the day and across leaf positions showed no evident relationship with  $g_s$  variation.

### **Biomass, yield and yield components**

Biomass and yield data were obtained from two independent experiments at HOR. Between experiments, yields were 32% higher in the first season but this was not due to increased biomass accumulation, which was larger in the second season (+59%, Table 2). Between yield components, a non-significant trend showed that kernel number was more affected (−13%) than kernel weight (−4%) in the second season compared with the first season.

Increasing plant density from 5.7 to 8.6 plants  $\text{m}^{-2}$  did not improve yield or modified yield components in 2019–20, whereas in 2020–21 a +26% yield gain was obtained by increasing plant density in both genotypes (Table 2). This was related to a +28% increase in kernel number that did not substantially affect kernel weight (−4%) and with +22% biomass accumulation. Comparing genotypes, white corn exhibited constitutively higher kernel weights and a non-significant trend to higher yields across seasons and plant densities (Table 2). Thus, yield benefits were obtained by increasing plant density in the second season, when overall lower temperatures were experienced and lower yields were attained.

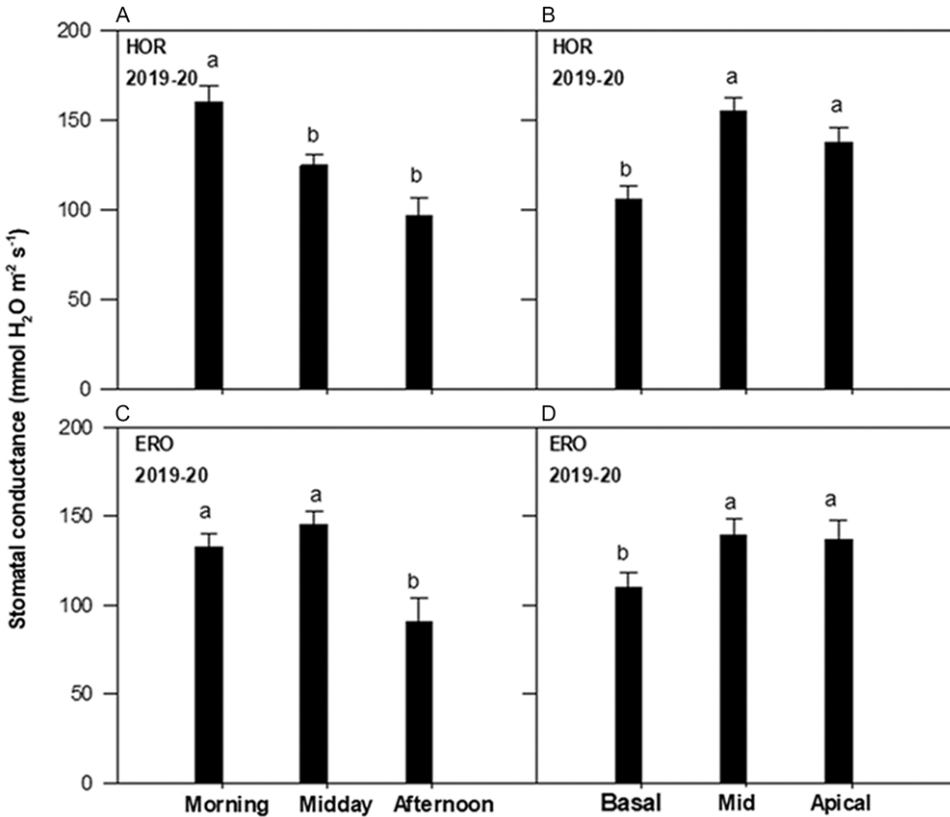


**Figure 4.** Stomatal conductance (mmoles H<sub>2</sub>O m<sup>-2</sup> s<sup>-1</sup>) at the same leaf spot where photosynthetic electron transport rate measurements were taken in Andean maize at Hornillos (2365 masl, a, b) and at El Rosal (3350 masl, c, d) during 2019–20. In each site, measurements were taken during 2 consecutive days, in the morning, midday and afternoon, in plants grown under two contrasting plant densities (5.7 plants and 8.6 plants m<sup>-2</sup>) and in 3 leaves representing different positions within the canopy. Significant differences during the day are shown in A and C by pooling together plant densities and leaf positions, whereas significant differences between leaf positions are shown in B and D by pooling together plant densities and time of the day. Lines above the bars indicate the standard error and letters show homogeneous groups according to the LSD test ( $p < 0.05$ ).

**Yield response to plant density in farmer’s fields**

Plant density and yield data were also obtained from samplings in 8 farmer’s fields within an altitudinal range spanning from 2400 up to 3400 masl during the 2022–23 growing season. A wide range of plant densities were explored across farms, with a minimum of 6 and a maximum of 15 pl m<sup>-2</sup>. The expected significant relationship between plant density and yield per plant was found (Fig. 5a,  $r^2 = 0.57^{***}$ ). Based on the linear equation obtained from this relationship, it was possible to estimate an expected yield per plant at each density and with this an optimum yield of 3650 kg ha<sup>-1</sup> was achieved at 10 pl m<sup>-2</sup> (inset in Fig. 5a). Regarding yield components, kernel number m<sup>-2</sup> was positively related to plant density ( $r^2 = 0.40^{**}$ , Fig. 5b) with no evidence of stagnation even at 15 pl m<sup>-2</sup>. By contrast, kernel weight was negatively related to plant density ( $r^2 = 0.41^{**}$ , Fig. 5c). Data belonging to highest altitude locations (empty symbols in Fig. 5) are usually located above the trend line in Fig. 5b and below the trend line in Fig. 5c, suggesting that, as altitude increases, increasing plant densities result in relatively higher gains in grains m<sup>-2</sup> and higher penalties over kernel weight. Thus, in these high-altitude environments, kernel weight is the yield component clearly most affected by increases in plant density whereas no apparent detrimental effect is seen for kernel number even at very high plant densities as 15 pl m<sup>-2</sup>.

**Table 2.** Yield (kg ha<sup>-1</sup>), kernel number (KN m<sup>-2</sup>), kernel weight (KW, mg kernel<sup>-1</sup>) and biomass (kg ha<sup>-1</sup>) in two genotypes of Andean maize (white and yellow corn) grown at Hornillos (HOR, 2380 masl) during 2019–20 and 2020–21 under two contrasting plant densities (5.7 and 8.6 pl m<sup>-2</sup>). Statistical significance represented as: +: *p* < 0.1; \*: *p* < 0.05; \*\*: *p* < 0.01 and \*\*\*: *p* < 0.001; NS indicates no significant relationship. For each trait, mean values for each significant factor or interaction among factors are deployed

	Yield (kg ha <sup>-1</sup> )	KN m <sup>-2</sup>	KW (mg kernel <sup>-1</sup> )	Biomass (kg ha <sup>-1</sup> )
<i>Experiment</i>				
I	6356 a	1304	511	16 100
II	4821 b	1152	491	25 624
<i>Plant density</i>				
5.7	5245	1091	506	21 233
8.6	5713	1296	487	24 820
<i>Genotype</i>				
Yellow	5251	1274	433 b	22 573
White	5707	1112	560 a	23 480
<i>Experiment * Plant density</i>				
I 5.7	6546 a	1301 ab	522	16 230 c
I 8.6	6166 ab	1307 ab	501	15 970 c
II 5.7	4270 c	1012 a	500	23 109 b
II 8.6	5373 b	1292 b	482	28 138 a
<i>Plant density * Genotype</i>				
5.7 Yellow	5058	1123	443	21 164
5.7 White	5432	1059	569	21 302
8.6 Yellow	5443	1425	424	23 982
8.6 White	5983	1166	550	25 657
<i>Experiment</i>	***	NS	NS	***
<i>Plant density</i>	NS	NS	NS	*
<i>Genotype</i>	NS	NS	***	NS
<i>Experiment × Plant density</i>	*	+	NS	*
<i>Experiment × Genotype</i>	NS	NS	NS	NS
<i>Plant density × Genotype</i>	NS	NS	NS	NS
<i>Experiment × Plant density × Genotype</i>	NS	NS	NS	NS

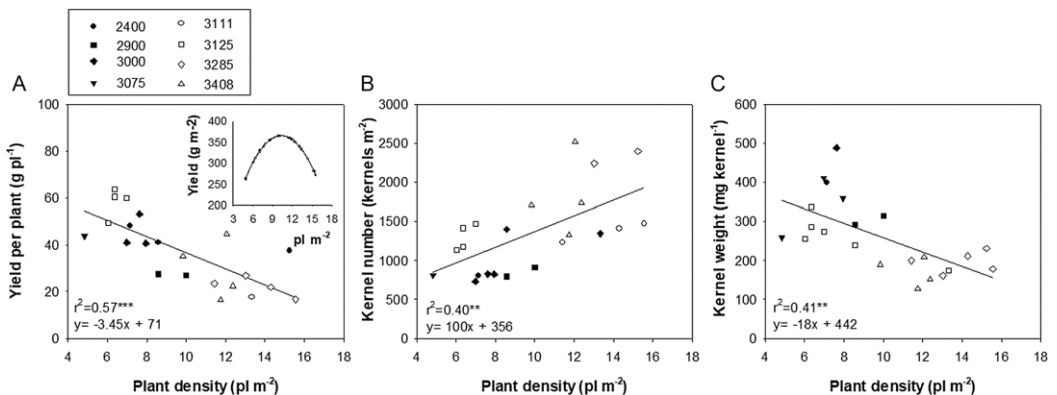


**Figure 5.** Results obtained from samplings in farmer’s fields during 2022–23 growing season: yield per plant (A), kernel number m<sup>-2</sup> (B) and kernel weight (C) as a function of plant density (estimated by the number of plants in the sampled row and the adjacent rows at each side). Different symbols denote the altitude of each location, whereas each symbol represents the average value of each sampled row (1.5 m length). Inset in (A) shows the expected yield response based on the linear equation obtained between yield per plant and plant density. Asterisks denote significant regressions: \*\*, *p* < 0.01; \*\*\*, *p* < 0.001.

## Discussion

### **Phenological development**

As expected, the lower temperatures associated with increased altitude at ERO had an important effect in delaying crop phenology, with 39 additional days being required to achieve R1 compared with HOR. Similarly, for landraces grown in Mexico in sites at 1550 and 2050 masl, up to 50 extra days were required to achieve the V16 stage at 2050 masl (Pace, 2019). However, these extra days did not fully compensate for growing degree days: 297°C.d less was required to achieve the R1 stage at ERO compared with HOR in our work. Similarly, 200°C.d less was required to complete the crop cycle in sites with the same photoperiod and differing in only 400 m of altitude (Jiang *et al.*, 1999). This is consistent with environmental modulation of the plastochron (Padilla and Otegui, 2005) and the phyllocron in maize (Riva-Roveda *et al.*, 2016; Tsimba *et al.*, 2013a). The phyllocron is decreased with lower temperatures within the range of 12.5–25.5°C (explored in our study) and also by increased solar radiation (Birch *et al.*, 1998), whereas higher proportion of UV-B apparently does not affect development (Kakani *et al.*, 2003). Overall, the increase in altitude delayed phenological development but also, drastically reduced the thermal time requirements in the maize genotype studied in our work.

### **Leaf area index and light interception improved at higher density**

Leaf area index and light interception were greatly reduced at the highest altitude site in line with previous reports (Cooper, 1979). While both delayed phenological development and reduced leaf size could account for these differences, here, leaf size was higher at ERO, at least for early-developed leaves (Fig. S2), which has been explained as a result of prolonged duration of leaf expansion (Cooper, 1979; Laffitte and Edmeades, 1997). Nonetheless, very low temperatures were explored in our work at the highest altitude site (>90 days with minimum T below 10°C during the vegetative period, Fig. 1b) and relatively mild chilling temperatures (14/10°C) can reduce leaf size both through effects over cell division and expansion (Louarn *et al.*, 2010). Thus, both effects, prolonged duration of leaf expansion and chilling affecting leaf expansion are likely interacting in opposite directions, finally increasing (as here) or decreasing leaf size at higher altitudes.

The increase in plant density improved light interception by 75 DAS at ERO (Fig. 2b), and until 78 DAS at HOR in the second season (Fig. 2d), which coincided with the crop achieving a LAI of 4 at low density (Fig. 2c), around the critical value for maize. Lower temperatures during the vegetative period at ERO (Fig. 1b), or a shorter vegetative period at HOR also combined with slightly lower temperatures (Fig. 1c), limited canopy development allowing plant density advantages in LAI and light interception to be expressed. By contrast, during 2019–20 at HOR, higher temperatures and a longer duration of the vegetative period (Fig. 1a) allowed a larger canopy to be developed, with no advantages of increased plant density related to a trend to reduced leaf size (not shown). Previous works have shown that leaf size is reduced with increasing plant density, but still, LAI usually increases up to 10–12 plants m<sup>-2</sup> except in very specific genotype × environment combinations (Madonni *et al.*, 2001). Thus, in these high-altitude environments, increasing plant density can improve LAI and light interception during the vegetative period, especially under cooler temperatures (ERO 2019–20) or shorter vegetative periods (HOR 2020–21) than those experienced at HOR 2019–20.

### **Leaf traits**

Many leaf traits changed between sites and plant densities. Overall, thicker leaves were attained at ERO (at high density, Table 1), which was not an outcome of decreased leaf size (Fig. S2). Consistent with this, specific leaf area is decreased in leaves developed at low T (Riva-Roveda *et al.*, 2016; Zhou *et al.*, 2020) and in maize lines from cool temperate regions compared with lines from

warmer origin (Verheul *et al.*, 1996). Increased light penetration in the canopy could explain the thicker leaves at ERO, whereas, at HOR, increased shading resulted in higher specific leaf area (Yabiku *et al.*, 2020) further augmented by high plant density (Table 1) in line with other works (Yang *et al.*, 2022). Other factors could also be involved, such as increased leaf sugar accumulation and decreasing specific leaf area which has been reported in leaves developed under lower T (Riva-Roveda *et al.*, 2016).

Higher SPAD values (+36%) and N contents on a dry mass basis (+39%) were achieved at ERO compared to HOR (Table 1), which was not simply an outcome of thicker leaves since relative differences for specific leaf area were much lower (8% higher at HOR). Low temperatures usually decrease chlorophyll and N content in maize (Nie *et al.*, 1995; Leipner *et al.*, 1997; Pasini *et al.*, 2005) and thus are unlikely to explain differences between sites in our work. By contrast, increased exposure to UV-B radiation results in higher chlorophyll concentration (Jovanić *et al.*, 2022; Zanca *et al.*, 2006) and leaf protein concentration (Tevini *et al.*, 1981), although these works did not explore the interaction with low T. Further work is needed to better assess the potential effects of UV-B radiation combined with lower temperatures over leaf traits, using realistic conditions as found in a high-altitude environment as ERO. In any case, thicker leaves, with higher protein content as found in ERO, could partially compensate for the decreased LAI with a higher photosynthetic potential.

### **Photosynthesis and stomatal conductance**

Photosynthesis was estimated through ETR, which in  $C_4$  species correlates closely with  $CO_2$  assimilation (Earl and Tollenaar, 1999). Because our measurements were made at full irradiance, the ETR obtained here is a proxy of the photosynthetic potential of the leaves in each treatment and condition. At HOR, ETR was unchanged throughout the day (Fig. 3a) with minimum T during the days of measurement always above 15°C (Fig. 1a). By contrast, at ERO, ETR progressively increased throughout the day, with 37% higher ETR in the afternoon compared with the morning (Fig. 3c) and minimum T during the days of measurements below 8.3°C (Fig. 1b). Consistent with this, low night T (<10°C) can reduce maize photosynthesis by up to 30% (Dwyer and Tollenaar, 1989; Ying *et al.*, 2000), chlorophyll fluorescence parameters such as ETR being directly affected (Ying *et al.*, 2000). On the basis of maximum ETR achieved at each site, leaves at ERO showed a higher photosynthetic potential and no penalties for increased plant density.

Our results also suggest that the rate of recovery from low night T could be slow at high-altitude sites such as ERO (highest ETR in the afternoon, Fig. 3c), with implications over photosynthetic water use efficiency (*i.e.* the quotient between photosynthesis and transpiration rate), as at the same location, maximum  $g_s$  was achieved in the early morning (+60% compared with the afternoon, Fig. 4c). Exploring genotypic differences in rates of recovery from low night T deserves further attention considering the potential implications on water use efficiency in these irrigated cropping systems. On the other hand, our results show that highest ETR rates were achieved at the highest altitude site (Fig. 3a vs. 3c in the afternoon) at very similar stomatal conductance rates (Fig. 4a vs. 4c in the afternoon), suggesting that the decrease in  $CO_2$  partial pressure with increasing altitude (Körner, 2007) was not a major constrain here.

### **Biomass, yield and yield components**

It is generally accepted that environments with a higher yield potential require higher planting densities to optimise yields (Tokatlidis *et al.*, 2011). However, there are some exceptions to this rule. For example, in late sowings, maize yields are usually decreased but optimum plant density can be similar or even higher compared with earlier sowings (Djaman *et al.*, 2022; Zhai *et al.*, 2021). In our work, higher yields were achieved in the first experiment at HOR but no response to plant density was obtained (6356 kg ha<sup>-1</sup>, Table 2), whereas in the second experiment, a later

sowing date combined with cooler temperatures and lower solar radiation likely resulted in lower yields ( $4821 \text{ kg ha}^{-1}$ , Table 2) but also in a positive response to increased plant density (+26% in both genotypes). Results obtained from farmer's fields (between 2400 and 3400 masl, thus higher than HOR) showed a consistent response of yield per plant to increasing plant densities (Fig. 5a), with an estimated maximum yield of around  $3600 \text{ kg ha}^{-1}$  being achieved at  $10 \text{ pl m}^{-2}$  (inset in Fig. 5a). Thus, environments with a lower yield potential (either in our second experiment or in farmer's fields) seemed to benefit by increases in plant density.

The yield improvement at high planting density in the second season was mostly related to kernel number  $\text{m}^{-2}$  (+28%) (Table 2) and was consistent with the larger LAI and light interception achieved before flowering at high density (Fig. 2c, 2d). Similarly, across farmer's fields, kernel number  $\text{m}^{-2}$  steadily increased with higher plant density (up to  $15 \text{ pl m}^{-2}$ ), with higher altitude locations being usually above the trend line (Fig. 5b). Benefits from increasing plant densities may be, thus, larger under higher altitudes (as it occurs in cool environments, Westgate *et al.*, 1997), improving radiation interception during the critical period, and with this, kernel number (Andrade *et al.*, 1999). On the other hand, reductions in kernel number at low planting density could be compensated for by larger kernels. But this was not observed, either in our second experiment (Table 2) or across farmer's fields, where at low planting densities, empty symbols (obtained from higher altitudes) usually located below the trend line (lower ability to compensate low planting densities with higher grain weights, Fig. 5c). According to Zhou *et al.* (2017), low minimum T ( $<20.7^\circ\text{C}$ ) during grain filling combined with a high daily thermal amplitude ( $T_{\text{max-min}} > 7^\circ\text{C}$ ) can decrease kernel growth rate. In our second experiment, minimum T during the first 30 days after silking was much lower than these ( $<10.8^\circ\text{C}$ ) and the daily thermal amplitude was much higher ( $T_{\text{max-min}} > 12^\circ\text{C}$ ). The same can be speculated for the higher altitude locations where samplings in farmer's fields were carried out. Consistently, dry matter remobilisation from vegetative parts is affected when ear T drops below  $16^\circ\text{C}$  (Setter and Flannigan, 1986), possibly explaining the coexisting low yields with high biomass accumulation in the second season. Thus, increasing plant density could be a promising strategy for improving yields in high-altitude environments. Further research is needed to understand mechanisms behind penalties on kernel weight; especially, whether higher kernel number can improve biomass allocation to the ear under low temperatures that limit kernel growth rates.

### Concluding remarks and future prospects

In this work, we show that increased altitude in mid-latitude environments of the Northwest of Argentina (3350 masl compared to 2300 masl) drastically delays phenological development, reduces thermal time requirements and modifies leaf traits increasing leaf thickness and leaf nitrogen content. Whereas a higher photosynthetic potential could be achieved at the highest altitude site this may not be fully exploited due to inhibitory effects of low night T and, apparently, long times of recovery from night chilling. Yield data obtained from experiments at 2300 masl and across farmer's fields within 2400 and 3400 masl indicate that increased plant density beyond those currently recommended could potentially improve yields regardless of the environmental yield potential, with maximum yields of  $3650 \text{ kg ha}^{-1}$  achieved at  $10 \text{ pl m}^{-2}$ . The main penalties of increased plant densities are related to reductions in kernel weight. Further work is needed to explore the effects of different factors limiting kernel growth rates, such as low temperatures and early frosts, over plant density responses.

**Supplementary material.** To view supplementary material for this article, please visit <https://doi.org/10.1017/S0014479723000194>

**Acknowledgements.** We thank Aldo Palacios, Director of the School at El Rosal, for providing the piece of land for field trials. We are also grateful to the support staff at IPAF for helping with the crop management. We are deeply thankful to the farmers

who kindly allowed us to carry out the samplings in their fields, who are, right now like many others, standing up for their ancestral territories under the threat of uncontrolled lithium business.

**Financial support.** This work was partially funded by the Consejo Nacional de Investigaciones Científicas y Tecnológicas, CONICET (National Council of Scientific and Technological Research, PIP 11220210100007) and by the FAO Project PR-154, Fondo de Distribución de Beneficios del Tratado Internacional sobre los Recursos Fitogenéticos para la Alimentación y la Agricultura, TIRFAA (Benefit-sharing Fund of the International Treaty on Plant Genetic Resources for Food and Agriculture).

**Competing interests.** The authors declare none.

## References

- Acciaresi H.A., Tambussi E.A., Antonietta M., Zuluaga M.S., Andrade F.H. and Guamet J.J. (2014). Carbon assimilation, leaf area dynamics, and grain yield in contemporary earlier- and later-senescing maize hybrids. *European Journal of Agronomy* **59**, 29–38.
- Andrade F.H. (1995). Analysis of growth and yield of maize, sunflower and soybean grown at Balcarce, Argentina. *Field Crops Research* **41**, 1–12.
- Andrade F.H., Vega C., Uhart S., Cirilo A., Cantarero M. and Valentín O. (1999). Kernel number determination in maize. *Crop Science* **39**, 453–459.
- Antonietta M., Girón P., Costa M.L. and Guamet J.J. (2019). Leaf protein allocation across the canopy and during senescence in earlier and later senescing maize hybrids, and implications for the use of chlorophyll as a proxy of leaf N. *Acta Physiologiae Plantarum* **41**, 1–10.
- Birch C.J., Vos J., Kiniry J., Bos H.J. and Elings A. (1998). Phyllochron responds to acclimation to temperature and irradiance in maize. *Field Crops Research* **59**, 187–200.
- Cámara Hernández J., Miente Alzogaray A.M., Bellón R. and Galmarini A.J. (2011). *Native maize landraces from Argentina*. Buenos Aires: Editorial Facultad de Agronomía, Universidad de Buenos Aires.
- Cantarero M.G., Cirilo A.G. and Andrade F.H. (1999). Night temperature at silking affects set in maize. *Crop Science* **39**, 703–710.
- Chen Y., Xiao C., Chen X., Li Q., Zhang J., Chen F., Yuan L. and Mi G. (2014). Characterization of the plant traits contributed to high grain yield and high grain nitrogen concentration in maize. *Field Crops Research* **159**, 1–9.
- Cirilo A.G. and Andrade F.H. (1994). Sowing date and maize productivity: I. Crop growth and dry matter partitioning. *Crop Science* **34**, 1039–1043.
- Cooper P.J.M. (1979). The association between altitude, environmental variables, maize growth and yields in Kenya. *The Journal of Agricultural Science* **93**, 635–649.
- Djaman K., Allen S., Djaman D.S., Koudahe K., Irmak S., Puppala N., Darapuneni M.K. and Angadi S.V. (2022). Planting date and plant density effects on maize growth, yield and water use efficiency. *Environmental Challenges* **6**, 100417.
- Dwyer L.M. and Tollenaar M. (1989). Genetic improvement in photosynthetic response of hybrid maize cultivars, 1959 to 1988. *Canadian Journal of Plant Science* **69**, 81–91.
- Earl H.J. and Tollenaar M. (1999). Using chlorophyll fluorometry to compare photosynthetic performance of commercial maize (*Zea mays* L.) hybrids in the field. *Field Crops Research* **61**, 201–210.
- Fryer M.J., Oxborough K., Martin B., Ort D.R. and Baker N.R. (1995). Factors associated with depression of photosynthetic quantum efficiency in maize at low growth temperature. *Plant Physiology* **108**, 761–767.
- Gómez G.L. and Macedo M.R. (eds.) (2011) *The Maize Crop in Family Agriculture of Northwestern Argentina*, Proyecto Minifundio, ed. Tucumán: INTA.
- Gornitzky C. (2015). *Development, Security and Food Sovereignty. We Are the Earth*. Argentina: Ediciones INTA.
- Hirasawa T. and Hsiao T.C. (1999). Some characteristics of reduced leaf photosynthesis at midday in maize growing in the field. *Field Crops Research* **62**, 53–62.
- Jenkins G. I. (2017). Photomorphogenic responses to ultraviolet-B light. *Plant, Cell and Environment* **40**, 2544–2557.
- Jiang C., Edmeades G.O., Armstead I., Lafitte H.R., Hayward M.D. and Hoisington D. (1999). Genetic analysis of adaptation differences between highland and lowland tropical maize using molecular markers. *Theoretical and Applied Genetics* **99**, 1106–1119.
- Jovanić B.R., Radenković B., Despotović-Zrakić M., Bogdanović Z. and Barać D. (2022). Effect of UV-B radiation on chlorophyll fluorescence, photosynthetic activity and relative chlorophyll content of five different corn hybrids. *Journal of Photochemistry and Photobiology* **10**, 100115.
- Kakani V.G., Reddy K.R., Zhao D. and Sailaja K. (2003). Field crop responses to ultraviolet-B radiation: a review. *Agricultural and Forest Meteorology* **120**, 191–218.
- Körner C. (2003). *Alpine Plant Life*, 2nd Edn. Berlin: Springer, 344 pp.
- Körner C. (2007). The use of 'altitude' in ecological research. *Trends in Ecology and Evolution* **22**, 569–574.



- Kosová K., Haisel D. and Tichá I.** (2005). Photosynthetic performance of two maize genotypes as affected by chilling stress. *Plant Soil and Environment* **51**, 206–212.
- Lafitte H.R. and Edmeades G.O.** (1997). Temperature effects on radiation use and biomass partitioning in diverse tropical maize cultivars. *Field crops research* **49**(2-3), 231–247.
- Leipner J., Fracheboud Y. and Stamp P.** (1997). Acclimation by suboptimal growth temperature diminishes photooxidative damage in maize leaves. *Plant, Cell and Environment* **20**, 366–372.
- Li C., Xiong Y., Cui Z., Huang Q., Xu X., Han W. and Huang G.** (2020). Effect of irrigation and fertilization regimes on grain yield, water and nitrogen productivity of mulching cultivated maize (*Zea mays* L.) in the Hetao Irrigation District of China. *Agricultural Water Management* **232**, 106065.
- Louarn G., Andrieu B. and Giauffret C.** (2010). A size-mediated effect can compensate for transient chilling stress affecting maize (*Zea mays*) leaf extension. *New Phytologist* **187**, 106–118.
- Maddonni G.A., Otegui M.E. and Cirilo A.G.** (2001). Plant population density, row spacing and hybrid effects on maize canopy architecture and light attenuation. *Field Crops Research* **71**, 183–193.
- Montgomery E.G.** (1911). Correlation studies in corn. *Nebraska Agricultural Experiment Station Annual Report* **24**, 108–159.
- Muchow R.C., Sinclair T.R. and Bennett J.M.** (1990). Temperature and solar radiation effects on potential maize yield across locations. *Agronomy Journal* **82**, 338–343.
- Nie G.-Y., Robertson E.J., Fryer M.J., Leech R.M. and Baker N.R.** (1995). Response of the photosynthetic apparatus in maize leaves grown at low temperature on transfer to normal growth temperature. *Plant, Cell and Environment* **18**, 1–12.
- Pace B.A.** (2019). Physiology, photochemistry, and fitness of Mexican maize landraces in the Field (Doctoral dissertation, The Ohio State University).
- Padilla J.M. and Otegui M.E.** (2005). Co-ordination between leaf initiation and leaf appearance in field-grown maize (*Zea mays*): genotypic differences in response of rates to temperature. *Annals of Botany* **96**, 997–1007.
- Pasini L., Bruschini S., Bertoli A., Mazza R., Fracheboud Y. and Marocco A.** (2005). Photosynthetic performance of cold-sensitive mutants of maize at low temperature. *Physiologia Plantarum* **124**, 362–370.
- Ritchie J.T. and Nesmith D.S.** (1991). Temperature and crop development. *Modeling Plant and Soil Systems* **31**, 5–29.
- Ritchie S.W. and Hanway J.J.** (1989). How a corn plant develops (No. REP-11237. CIMMYT).
- Riva-Roveda L., Escala B., Giauffret C. and Périlleux C.** (2016). Maize plants can enter a standby mode to cope with chilling stress. *BMC Plant Biology* **16**, 1–14.
- Rosenqvist E. and Kooten O.V.** (2003). Chlorophyll fluorescence: a general description and nomenclature. In *Practical Applications of Chlorophyll Fluorescence in Plant Biology*. Boston, MA: Springer, pp. 31–77.
- Setter T.L. and Flannigan B.A.** (1986). Sugar and starch redistribution in maize in response to shade and ear temperature treatment. *Crop Science* **26**, 575–579.
- SOLCAST** (2022). Available at <https://solcast.com/>.
- Tevini M., Iwanzik W. and Thoma U.** (1981). Some effects of enhanced UV-B irradiation on the growth and composition of plants. *Planta* **153**, 388–394.
- Tokatlidis I.S., Has V., Melidis V., Has I., Mylonas I., Evgenidis G., Copandean A., Ninou E. and Fasoula V.A.** (2011). Maize hybrids less dependent on high plant densities improve resource-use efficiency in rainfed and irrigated conditions. *Field Crops Research* **120**, 345–351.
- Tokatlidis I.S. and Koutroubas S.D.** (2004). A review of maize hybrids' dependence on high plant populations and its implications for crop yield stability. *Field Crops Research* **88**, 103–114.
- Tsimba R., Edmeades G.O., Millner J.P. and Kemp P.D.** (2013a). The effect of planting date on maize: phenology, thermal time durations and growth rates in a cool temperate climate. *Field Crops Research* **150**, 145–155.
- Tsimba R., Edmeades G.O., Millner J.P. and Kemp P.D.** (2013b). The effect of planting date on maize grain yields and yield components. *Field Crops Research* **150**, 135–144.
- Utrillas M.P., Marín M.J., Esteve A.R., Salazar G., Suárez H., Gandía S. and Martínez-Lozano J.A.** (2018). Relationship between erythral UV and broadband solar irradiation at high altitude in Northwestern Argentina. *Energy* **162**, 136–147.
- Verheul M.J., Picatto C. and Stamp P.** (1996). Growth and development of maize (*Zea mays* L.) seedlings under chilling conditions in the field. *European Journal of Agronomy* **5**, 31–43.
- Waqas M.A., Wang X., Zafar S.A., Noor M.A., Hussain H.A., Azher Nawaz M. and Farooq M.** (2021). Thermal stresses in maize: effects and management strategies. *Plants* **10**, 293.
- Westgate M.E., Forcella F., Reicosky D.C. and Somsen J.** (1997). Rapid canopy closure for maize production in the northern US corn belt: radiation-use efficiency and grain yield. *Field Crops Research* **49**, 249–258.
- Wilkens P. and Singh U.** (2003). A code-level analysis for T effects in the CERES models. Modeling T Response in Wheat and Maize. El Batán, Mexico, 1–7.
- Yabiku T., Akamatsu S. and Ueno O.** (2020). Light reacclimatization of lower leaves in C<sub>4</sub> maize canopies grown at two planting densities. *Photosynthetica* **58**, 732–739.
- Yang K., Chen G., Xian J. and Chen W.** (2022). Varying relationship between vascular plant leaf area and leaf biomass along an elevational gradient on the Eastern Qinghai-Tibet plateau. *Frontiers in Plant Science* **13**, 824461.

- Ying J., Lee E.A. and Tollenaar M.** (2000). Response of maize leaf photosynthesis to low T during the grain filling period. *Field Crops Research* **68**, 8796.
- Zancan S., Cesco S. and Ghisi R.** (2006). Effect of UV-B radiation on iron content and distribution in maize plants. *Environmental and Experimental Botany* **55**, 266–272.
- Zhai L., Zhang L., Yao H., Zheng M., Ming B., Xie R., Zhang J., Jia X. and Ji J.** (2021). The optimal cultivar× sowing date× plant density for grain yield and resource use efficiency of summer maize in the northern Huang–Huai–Hai Plain of China. *Agriculture* **12**, 7.
- Zhou B., Yue Y., Sun X., Ding Z., Ma W. and Zhao M.** (2017). Maize kernel weight responses to sowing date-associated variation in weather conditions. *The Crop Journal* **5**, 43–51.
- Zhou H., Zhou G., He Q., Zhou L., Ji Y. and Zhou M.** (2020). Environmental explanation of maize specific leaf area under varying water stress regimes. *Environmental and Experimental Botany* **171**, 103932.

---

**Cite this article:** Salve DA, Maydup ML, Salazar GA, Tambussi EA, and Antonietta M. Canopy development, leaf traits and yield in high-altitude Andean maize under contrasting plant densities in Argentina. *Experimental Agriculture*. <https://doi.org/10.1017/S0014479723000194>